Egypt. J. Chem. **Vol. 66,** No. 6 pp. 159 - 169 (2023)

Egyptian Journal of Chemistry

http://ejchem.journals.ekb.eg/

Green Synthesis of Iron Nanoparticles Loaded on Bovine Lactoferrin Nanoparticles Incorporated into Whey Protein Films in Food Applications

Lames Thamer Alhadide[a] , Zaizafoon N. Nasif [b] , Muntadhar S.Sultan[b]

[a] *Collage of agriculture and engineering science, University of Baghdad-Iraq*

[b] *Chemistry department, science collage , Mustansiriyah university-Iraq*

Abstract

Since nanotechnology offers a "different stage" followed by fresh or altered properties imposed on many existing products, it is commonly used in the manufacture of drug formulations of a new generation and is also used in the food industry as well as in many types of nutritional supplements. The synthesized iron oxide Fe_2O_3-NPs (IONPs) and bLf nanoparticles (0.2 percent, w / v) were successfully generated by thermal gelation (75 ° C for 20 min). The NPs were examined by UV / Vis absorption spectroscopy, transmission electron microscopy TEM. A typical absorption peak of iron oxide nanoparticles that synthesized (by using *CONCARPUS* extract as reducing agent) appear at range of 200-300 nm and 200-400 nm of blfNPs and IONPs carried on blfNPs respectively which observed by color transformed from transparent yellow to black, demonstrating the synthesis of iron nanoparticles. The total particle size of prepared IONPs, blfNPs and IONPs carried on blfNPs was 80 nm, 60 nm and 200 nm, respectively. Mechanical test of prepared films appeared that increasing NPs ratio resulted in the decreases in the film thickness, tensile strength (TS), and elongation at break (EAB), O_2 permeability, water vapor permeability and decreased the film solubility. The antimicrobial efficacy of the prepared nanoparticles in combination with the manufactured whey protein films was investigated using the well diffusion technique versus harmful *S.aureus*, *S.agalactiae*, *E.coli*, and *Salmonella enterica*. Antioxidant activity of extracts and prepared films 5%, 10%, 15% of blfNP loaded IONPs were expressed as percentage of DPPH radicals' inhibition percentage. Values in percentage ranged from 70.1, 74.59, 76.41 ,79 %. The total phenolic content ranged from (6.6,7.1,7.6,7.9 mg/g of sample) for plant extract and prepared films5%, 10%, 15% of blfNP loaded IONPs respectively, expressed as gallic acid equivalents. This approach to biosynthesis for applications has been found to be cost-effective, environmentally sustainable and promising in different fields. Overall, findings indicated that bLf nanoparticles loaded IONPs combined with whey protein film may be used for potential food applications.

keywords: Concarpers leaves, Iron oxide nanoparticles, Lactoferrine nanoparticles, Whey protein films;

1. Introduction

More natural and biodegradable materials is need for goods grows, food industry as their possible improvement in food packaging [1]. The bulk of existing materials used in the packaging industry are made from fossil fuels and are non-degradable [2].

Pollution and increased nutrient shelf-life have encouraged the discovery of modern bio based products [3]. Biologically determined wrapping consists of raw derived from ecological importance, implying that the package is made of organically, biological components and contains edible films and also composites of primary and secondary wrapping ingredients [4]. Several researchers have documented the green synthesis of iron nanoparticles using different plant extracts [5], the simplest, most cost-effective and reproducible technique is to synthesize metallic nanoparticles from different plant components such as leaves, stem, seed and core due to presence of various organic reduction compounds in the plants [6, 7]. Various herbs and plant products produce higher antioxidants, which are present in grains, vegetables, leaves and stems as phytochemical constituents [8]. The Green synthesis of iron nanoparticles (Fe NPs) was carried out mainly using green tea extract, which is a cheap and local tool [9]. Aqueous extracts of *Sageretia thea* (Osbeck) containing a variety of polyphenols was used to synthesized zero valent iron nanoscale particles with distinctive properties [10]. Because an increasing number of bioactive components have been found in milk hydrolysates, milk proteins are recognized as the main essential reservoir of bioactive proteins. The potential nutrition advantages of milk protein-derived peptides in terms of health-promoting functional meals has piqued considerable interest [11]. Whey

*Corresponding author e-mail:.; lamesthamer7979@gmail.com (Lames Thamer Alhadide)

Receive Date: 26 July 2022, Revise Date: 13 August 2022, Accept Date: 05 September 2022

DOI: 10.21608/EJCHEM.2022.152557.6608

protein can be integrated into edible films that impart nutritious and functional properties as a byproduct of the dairy industry. The fractionated composition of whey proteins is β-lactoglobulin (β-Lg, 57%), alpha-lactoalbumin (alpha-La, 19%), bovine serum albumin (BSA, 7%), immunoglobulins (Igs, 13%) and unique polypeptides (PP, 4 percent). Whey protein (WPI) is used to produce an extremely concentrated whey protein substance (90-95 percent protein) by ultra-filtration and ion-exchange, the main fraction being β-Lg. For WPI, many functional properties such as emulsifying foaming, gelling and barrier agents have been identified [12]. Lactoferrin (formerly known as lactotransferrin) is a glycoprotein and a part of a class of transferrins, thus belongs to certain proteins capable of attaching and transmitting Fe^{3+} ions. Subsequent studies detected lactoferrin in exocrine gland secretions and in particular neutrophil granules [13]. Neutrophils were shown to be the key source of lactoferrin in the blood plasma after degranulation owing to its elevated production during most inflammatory reactions and certain viral infections, some scholars recognize lactoferrin as an acute-phase protein [14, 15]. The association between its exposure and physiological or adverse impact on body functions, though, is still not well characterized [16] .This phenomenon recalls the interactions which have been observed between lactoferrin and other important immunological factors [17]. As pointed out by [17], several investigators have noted the joint presence of lactoferrin and lysozyme in milk,specific granules of polimorphonucleates, tears and tubotympanum mucus. And in in vitro tests a synergy between lactoferrin and lysozyme was shown towards various bacteria [18]. Moreover, in the past it was observed that lactoferrin may act synergistically with complement and with antibodies [19].

The purpose of this study is to establish and describe bovine lactoferrin (bLf) nanomaterials as an iron carrier, as well as to find the optimal base material and plasticizer for the production of whey protein films with different physical and chemical characteristics.

2. Materials and Methods

The chemicals $FeCl_3$, NaOH, glycerol and HCl were supplied by Merck, India Ltd. Nutrient agar and MacConkey agar was obtained from Himedia Pvt. India, Ltd. *CONCARPUS* leaves was collected from Palestine Street / Baghdad province for extract preparation. DMV International (USA) had distilled bLf material. Its powder produced (expressed as a percentage of dry weight) 96 percent protein, 0.5 percent dirt, 3.5 percent moisture and 0.012 percent iron (manufacturer's data). Iron chloride ($FeCl_3$) was collected from Panreac (Barcelona, Spain) (97% purity). Phosphate buffer saline (PBS) and hydrochloric acid (HCl) (36.5–38.0 percent purity), Folin-Ciocalteu reagent, galic acid DPPH, vitamin C were supplied by Sigma – Aldrich Chemical Co. Ltd. KCl and NO (35% purity) obtained from Merck (Darmstadt, Germany); sodium hydroxide (NaOH) obtained from Fisher Science (UK).

2.1. *Preparation of Concarperes leaves sheath extract*

To avoid the dust and other particulate matter, *CONCARPUS* leaves sheath were gathered and washed vigorously in water. Fine sheath pieces in water (200 g/L) were put in soxhlet at 60° for 24 h. During soxhlet extraction, distillation phase was involve [20]. This process is done continuously until the extraction is completed [20]. Separation of the extract into the solvent is performed using the Rotary evaporator unit. For more tests the extract was kept at 4 °C.

2.2. *Preparation of IONPs*

Dissolving the $FeCl_3$ in purified water has produced a solution of $FeCl_3$ (5 mM). *CONCARPUS* leaves extract was used in a standard green synthesis procedure to minimize and cap the Fe ions. At normal atmospheric pressure, In the aqueous $FeCl_3$ solution, 10 ml of extract was added. The solution was mixed for 8 h at 70-80 °C for 24 hrs. UV-Vis area reported maximum absorption wavelengths of iron colloids (from 200 nm to 800 nm) [21].

2.3. *bLf NPs preparation: Protein solution preparation*

In short, 0.2 percent (w/v) of the bLf solution was dissolved for 1 h during agitation in distilled water at 25 °C. According to Martins et al., the pH of the items is then used with 1 M NaOH and/or 1 M HCl changed to 7 as required. Protein solutions (0.2 percent bLf, pH 7) are suitable for the production of nanoparticles under varying thermal conditions (i.e., 75 °C and a holding time of 20 min), combining 40 mM of previously prepared IONPs [23].

2.4. *Spectrophotometric study of IONPs using UV-Vis*

The synthesis of Fe_2O_3NPs, blf NPs and blfNP loaded Fe_2O_3 NPs was tentatively verified by reporting up to 200-800 nm of absorbance in UV-Vis spectra. The UV-Vis spectrophotometer was used to record changes in the surface plasmon resonance (SPR) of nanoparticles during dispersion.

2.5. *Transmission electron microscopy (TEM) measurement*

A Zeiss EM 902 A (German) instrument was used to examine the morphological characteristics of iron NPs, blf NPs, and iron-coated bLf nanoparticles with or without iron. In coated carbon copper grids, the specimens were attached and air - dried at room temperature.

2.6. *Antimicrobial Activity Test of IONPs, blfNPs, blfNPs loaded with IONPs*

Antimicrobial property of synthesized Fe_2O_3-NPs was tested to explore the herbal functionality of NPs. Antimicrobial activity was determined by agar well diffusion method. For antibacterial test the organisms used were 10 mL of bacterial suspension, Gram negative - Escherchia coli, Gram Positive- Staphylococcus aureus. H3 on Mueller–Hinton agar on age 24 hrs pour into the plates. Allow to set on a level surface, to a depth of approximately 6 mm as three pours position .Then three pours in Plates was loaded with 60 µL of IONPs , blfNPs , blfNPs loaded with INPs respectively, incubate fat 37° C for 24 hrs then measured inhibition diameters in mm [22].

2.7. *Preparation of Film Forming Suspensions*

A whey protein standard solution (WPSS) was formulated using the standard method defined by Popovi´c *et al* [23]. At the start, deionized water was used to dissolve 10% of WPI (w/w) at room temperature under continuous stirring (200 rpm) for half hour by using Thermomix 31-1 (Germany). The prepared solution was heated under the same stirring condition up to 90 °C for another half hour, therefore, the protein was denatured [19]. The next step was involved the sonication of the solution for cooling and degassing for 15 minutes by using a DT 514H ultrasonic bath (Germany). The mixture was uniformly mixed with upon cooling off, glycerol was added to the solution and the mixture was stirred with Thermo mix under 200 rpm for another half hour. Then the mixture was applied to another degassing sonication for 15 minutes. Next, the WPSS and the aqueous solution of iron were stirred with a magnetic bar (Ikamag, Germany) at 1200 rpm to achieve the dispersion of the suspension solution. The operation was proceeded for one hour on a loaded IONPs ratios of 5%, 10%, and 15% (w/w) with respect to the protein content to obtain the desired lactoferrin. The nano dispersion was added gradually under continuous stirring to prevent the agglomeration in the solution. Before it was mixed with WPSS, The nano dispersion was redispersed once more at room temp and sonicated then sonotrode for half hour at 500 rpm by using electric stirrer at 400W for 45 minutes [24].

2.8. *Preparation of whey protein films*

Glass plates with 15 cm diameter (about 8.5 cm^2), were used for preparation films. The 8 g of the film forming dispersions (FFDs) was cast in the center of glass plates and dried at 21º C for about 48 h (it was varied 24-40 h based on the kind of FFDs). Dried films are held at 25ºC and 50 % relative humidity (RH) before assessment [25].

2.9. *Mechanical properties*

1. **Film Thickness**: A portable micrometer (Mituto, Tokyo, Japan) with a sensitivity of 0.01 mm has been measured for film thickness. Measurements were made at various points (at least nine random locations) and findings were recorded for each film sheet as a mean and standard deviation [26].
2. **Water Solubility**: The solubility of film samples has been calculated using [26] process. The samples were cut into pieces with are of 3×2 cm and these pieces were used in the solubility test. The pieces were weighted by suing an electric balance and the weight was registered as W1, then the prices were dried in the oven at 105 ºC for one day. Then each piece was immersed in 10 mL deionized water in 50 mL tube. The tubes were held for one day in a shaker at room temperature. The solvent was purified and the traces were dried in an oven at 105o C for 24 hours on the filter paper after the samples were weighed to determine the water-soluble dry content (W2).
3. **Tensile strength (TS) and elongation at break (EAB):** TS and EAB were measured by means of a modified optical fruit sclerometer. On the mechanical fruit sclerometer handle, film strips (20 - 60 mm) were mounted. From the device's digital monitor, the maximum force needed for each film to rupture was read. The TS was measured by dividing the average force of rupture (F) and the film cross-section region (A) obtained by multiplying the film strip width and mean thickness. EAB was determined by comparing the change in film strip length after a breach occurred (b) with the original film strip length before loading (a) [27].
4. **Water vapor permeability:** EAB was determined by comparing the change in filmstrip length after a breach occurred (b) with the original filmstrip length before loading (a). [28]. ($CaCl_2$ - 0 percent RH) was completely filled within the cell, and the device was put in a desiccator with saturated (NaCl - 75 percent RH). The RH inside the cell was always smaller than outside, so water vapor movement was estimated at a steady state of change from the weight gain of the permeation cell conducted at 12 h intervals over a 7-day span up to the nearest 0.0001 g, and adjustments in cell weight were reported and plotted as time feature. The slope of each line (Microsoft ® Office Excel 2007) was estimated by linear regression and the rate of water vapor transfer (WVTR) from the slope (g H_2O/s) divided by the cell area (m^2) was determined. The WVP value is expressed as [g mm

m-2 d-1 kPa-1. For each type of film, the WVP was calculated in triplicates [27].

5. **Oxygen permeability:** In compliance with ASTM D3985, the oxygen transmission rate was calculated using the Ox-Tran modular method (Mocon, Inc., Minneapolis, MN, USA) at 23 ° C and 50 ± 1 per cent RH (ASTM, 2010). The samples were calibrated 48 h prior to review at 50 ± 1 per cent RH (23 ± 1 °C). The film samples were mounted on a mask of stainless steel with an open research area of 5 cm^2. Nitrogen gas, on one side of the film (98 percent N_2 and 2 percent H_2) flowed 100 percent oxygen gas on the other. To the coulometric sensor, nitrogen gas was conducted and measurements were obtained when a stable state was reached. A humidifier controlled the relative humidity of both gasses and ranged from 50 to 90 percent. The permeability study was not done below RH 50 percent because at such lower RH rates the starch films started cracking. The oxygen permeability was measured by measuring the O_2 emission rate by the partial pressure difference in O_2 between the two sides of the film (101 kPa) and multiplying by the mean thickness of the film (μm). The measurements were conducted in duplicate and the OP units were cm^3 μm m-2 d-1 kPa-1 kPa-1 [27].

2.10. *Effect of preparation film contains 5%, 10%, 15% of blfNP loaded IONPs on pathological bacteria bacterial strains*

Disc diffusion method: The film's antimicrobial activity Samples of blfNP loaded IONPs was calculated using the system of diffusion agar. Movie samples with a diameter of 10 mm were cut aseptically into disk form and then put on MHA surfaces, previously smeared with 10 mL of broth culture comprising around 108 CFU / mL of certain food pathogens. The plates have been 24 hours incubated at 37º C. Using a caliper, the inhibition zone diameter was measured to the nearest 0.02 mm. As inhibition, zone diameter was not the same in the whole area, an average of at least three diameters for each area was known as inhibition zone diameter. Antimicrobial index [30] of the film samples was measured based on the total area [29].

2.11. *Determination of Phenolic Contents in extract ,5%, 10%, 15% of blfNP loaded IONPs films*

Folin-Ciocalteu method [31] was used to investigate the total phenolic content of the samples. To build the standard curve, a series of gallic acid solution (0.2-1 mg/mL) were used. The method involved the addition of 1 mL of each sample of the study (100 μg/mL plant extract, and 5%, 10%, and 20% of film samples) to 2.5 mL of 10% of the working reagent. Next, 2 mL of 75% Na2CO3 were added to the mixture after 5 minutes from the last step, and incubated at 50 ºC for 10 minutes under discontinuous stirring. Once the time has ended, the tubes were let to cool down to the room temp and the absorbance was read at 765 nm by using UV-Vis spectrophotometer (UV-1800 Shimadzu, Japan). The results were expressed in milligram of gallic acid equivalent in gram of sample (mg GAE/g of sample).

2.12. *DPPH Radical Scavenging Activity of extract ,5%, 10%, 15% of blfNP loaded IONPs films*

The DPPH method [31] was used to determine the radical scavenging activity (RSA) of the plant extract and the prepared nanofilms, and consider the antioxidant properties of the samples. The method was standardized with (1mM) vitamin C. The procedure was simply proceeded by adding 2mL of (0.1 mM) DPPH solution to 2 mL of each sample (100 μg/mL of the plant extract in methanol, or 5%, 10% or 15% of the nanofilm solution). The tubes then let to stand in the dark for half hour and then the absorbance was read at 517 nm by using UV-Vi spectrophotometer against methanol as blank. The absorbance of DPPH alone was read as well as the control. The RSA% was calculated according to the following formula:

$$RSA\% = ((A° - A))/(A°) \times 100$$

where Aº is the absorbance of control; A is the absorbance of samples.

3. Results and Discussion

Chemical nanoparticles manufacturing necessitates the employment of a variety of chemical reducing reagents and precursor compounds. The use of phytoconstituents as reducing and capsizing compounds in the green synthesis of metallic nanoparticles is considered as a positive step toward producing nanoparticles in a more ecologically responsible and cost-effective manner. A standard change of the extract of the leaves and the aqueous $FeCl_3$ mixture color from dark yellowish gray to black was confirmed by Fe_2O_3-NPs NPs synthesis. This suggested the reduction of Fe_2O_3-NPs NPs to aqueous iron ions when added to *CONCARPUS* extract leaves and the color reaction is the result of excitation of surface plasmon vibration in metal nanoparticles .INPs have been successfully synthesized with the leaf extract *CONCARPUS* by Devatha *et al* [30, 32].The *CONCARPUS* leaf extract was prepared in water at a ratio of 1:10 w/v. The bio reduction of Fe ions in aqueous fluids was monitored by examination of the UV-Vis spectra. In order to explore the absorption spectrum of green synthesized Fe_2O_3NPs, UV-Vis spectral analysis was carried out at a wavelength range of 100-900 nm and absorption peaks at 250-350 nm levels were observed as a result of surface excitation plasmon vibrations in Fe_2O_3-NPs NPs. Forming of

Fe_2O_3-NPs NP is known to occur by complexion the Fe salts followed by capping Fe with phenolic compounds [32]. Such observations are fully in line with other published studies [31].

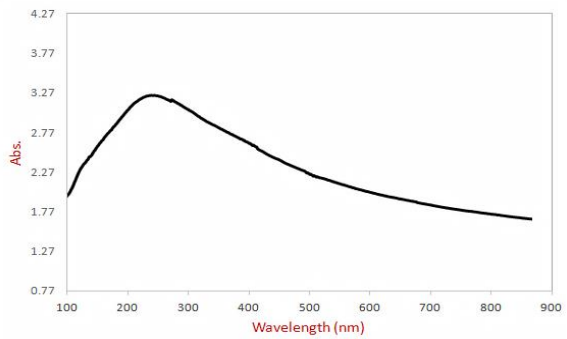

Figure 1. UV–Vis absorption spectra of Fe_2O_3-NPs.

Phytochemicals involve functional classes of hydroxyl, carboxyl, and amino, which may act both as efficient metal-reducing agents and as capping agents in a single phase to establish a protective coating on the metal nanoparticles, resulting in a color shift from yellowish brown to brownish black. This color change gave the confirmation of the synthesis of Fe_2O_3-NPs. This denotes the leaves of the *CONCARPUS* plant have premier competence to synthesize of Fe_2O_3-NPs than other parts of the plant such as seed, roots [32]. Morphologies of synthesized nanoparticles have been verified using HR-TEM analysis during bio-reduction (Figure 2). Spherical nanostructures with an average core diameter of 80 nm were shown by iron oxide nanoparticles and agglomeration of the particles was observed. A study [35] has recorded electron-dense particles of spherical iron oxide with a diameter up to 30 nm have been created [11].

In a recent report, Prasad et al. [36] formed nanocrystals of iron(III) oxide with Garlic Vine leaf extract and $FeCl_3$. Adding a few drops of 1 M NaOH has improved bio-precipitation. The reaction resulted in nanocrystals containing Fe_2O_3 with a scale of 18.22 nm. Lactoferrin seems to have tremendous promise in the therapeutic field because of its remarkable antimicrobial, antifungal, anticancer, and anti-inflammatory effects. It was used as a ligand to target various nanocarriers [33], But none of them used Lf as a matrix. The purpose of this study was to create and optimize Lf nanoparticles (LfNP) to improve the effectiveness of food storage in vitro. blfNPs are characterized by UV-Vis and TEM filled INPs. Their antimicrobial profile in vitro was studied. In addition to this, whey protein films and blfNPs loaded IONPs were prepared and characterized [34]. At a wavelength range of 100-900 nm, UV-Vis spectral analysis was conducted. The absorption peak of blfNPs was observed at 300 nm but the absorption spectra of blfNPs loaded INPs shifted to low absorbance due to decrease in excitation of surface plasmon vibrations which contribute to loss of α- helix content occur when protein are adsorbed with nanoparticles, with or without an increase in β-sheet, Figure 3.

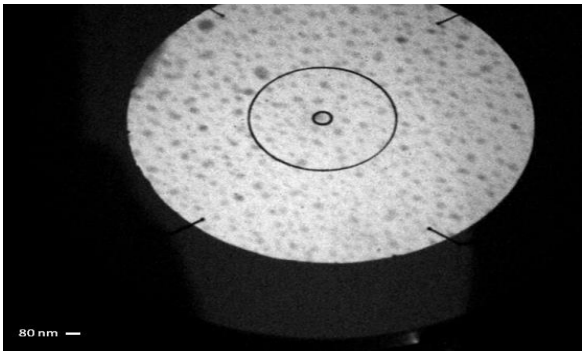

Figure 2. TEM of Fe_2O_3- NPs.

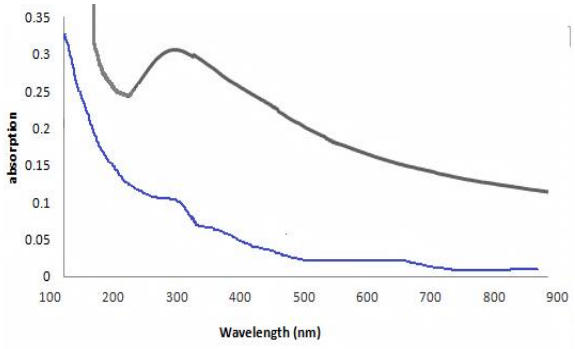

Figure 3. UV–Vis absorption spectra of blfNPs (black) and blfNPs loaded IONPs (blue).

TEM images (Figure 4) confirmed the production of bLf nanoparticles under the conditions studied (pH 7, 75 °C, 20 min and 35 mM $FeCl_3$) and composition values acquired (around 60 nm). There is also iron (black dots) shown in nanoparticles that show iron binding to bLf nanoparticles.

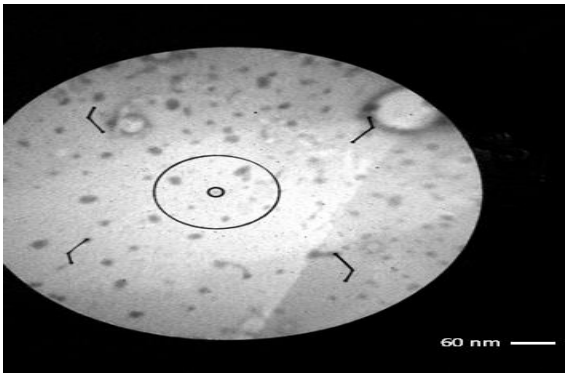

Figure 4. TEM of blf NPs.

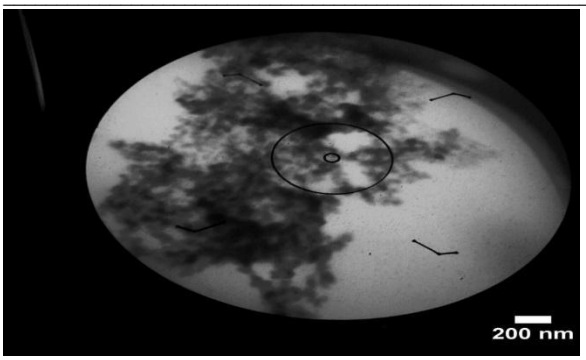

Figure 5. TEM of blf NP loaded on IONPs.

The TEM analysis revealed that blfNPs were in the range of 40-80 nm, with an average size of 60 nm (mean ±SD) for blank lactoferrin nanoparticles (figure 4) and in the range of 100-250 nm, with an average size of 200 nm (mean ±SD) for IONPs loaded lactoferrin nanoparticles (figure 5). It is apparent that lactoferrin nanoparticles become more than double in their average size after loading of the IONPs. Further, TEM analysis revealed that the nanoparticles were homogenous in their sizes and were spherical in their shapes. The isolated whey protein (WPI) films were clear, smooth, Flexible, homogenous and without the holes or gaps to be found. Changes were found in appearance for films inserted in Nanoparticles of 5%, 10% and 15% at various ultrasonic speeds.

Table 1 shows the typical film thicknesses, tensile and elongation of WPI films with and without nanoparticles. From Table 1 it is clear that adding nanoparticles reduces the thickness, tensile and elongation of cast films. In general, the same weight of film-forming fluid was casted onto 100 mm diameter petri plates, but with the inclusion of nanoparticles, the dry matter of the substances decreases [35]. If selecting a film for particular uses, water solubility of film forming components is an significant consideration. Indeed, solubility in many cases, such as food encapsulation, is a desired property. In Table 2, the water solubility of the WP films being made is seen. The effect of additives on film solubility is generally dependent on the shape and concentration of compounds and their underlying hyrophilic and hydrophobic indices. The solubility of a film is supposed to be improved by hydrophilic compounds, whereas hydrophobic compounds are expected to minimize it (40). Monitor solubility and composite films followed the same pattern as moisture content in the present research, which is in line with the assumption that increasing inclusion of various NP ratios will consequently minimize film hydrophilicity which contribute to loss ofα- helix content occur when protein is adsorbed with nanoparticles, with or without an increase in β-sheet.

Table 1 :Thickness, tensile and elongation % in different types of prepared films

Films types	Film Thickness (µ)	Tensile force (megapascal)	Elongation %	O_2 permbility mL/m2.day	Water permibility gm.mL/hr.day.megapascal
Control film	179	7.98	101	90.01	0.65
Film+ 5% lactoferrin NP loaded IONP	168	7.91	89.5	87.09	0.61
Film+ 10 % lactoferrin NP loaded IONP	161	7.86	87	82.55	0.55
Film+ 15% lactoferrin NP loaded IONP	155	7.83	86.4	79.34	0.49

Table 2:Solubility percentage of different types of prepared films in water

Films samples	% Film solubility in water
Control film	40.7
Film+ 5% lactoferrin NP loaded IONP	38.5
Film+ 10 % lactoferrin NP loaded IONP	37.2
Film+ 15% lactoferrin NP loaded IONP	35

when measuring WVP. The WVP depends on the amount of polar groups present in the protein film of whey is hydrophilic; it is extremely polar amino acid compound [36]. Furthermore, whey powder includes lactose fat, a strongly hydrophilic material [37]. Film's barrier properties are determined by the hydrophobic or Polymer hydrophilic form, appearance of film or hols. Form, quality and reliability of plasticizers integrated and steric video form hindrance. Cowpea protein denaturation in higher Hydrophilic residues are revealed to the protein surface by pH levels [38]. This increases absorption Migration of water molecules between polar pairs, allowing movement simpler of water and allowing further water vapor to enter by film [38]. The WVP of the improved whey protein film increased with an expanded ratio of IONPs filled by blfNPs [39]. Protein gelling is one of the most commonly employed Formgels are using techniques for the production of protein aggregates even at large concentration [40]. BLf nanoparticles can be useful for milk and pharmaceutical applications, e.g. for optical or rheological alterations of product properties or for encapsulation and supply of bioactive ingredients [41].

Antibacterial activity was tested against *Escherichia coli Salmonella spp. Pseudomonas aeuroginasa Staphylooccus aereus Bacillus spp Candida albicans* (As seen in Table 3), it was observed from the experiment that the iron nanoparticles have been successful in inhibiting bacterial evelopment. In IONPs the inhibition zone was decreased than blfNPs and lso in blfNP primed IONPs alone was decreased, the results indicate a high antibacterial potency of the iron nanoparticles and blfNPs loaded IONPs.

Table 4 concluded increasing the inhibition zone of bacteria with increasing the ratio of NPs added to whey protein films.

Table 3 :The inhibition effect (zones in mm) of IONPs, blf NPs and blf NP loaded on IONPs on variant type of micro-organism

Lactoferrin NP loaded IONPs	IONPs	lactoferrin	Micro-Organisms types
24	15	12	*Escherichia coli*
28	21	19	*Salmonella spp.*
23	19	17	*Pseudomonas aeuroginasa*
27	20	18	*Staphylooccus aereus*
29	21	19	*Bacillus spp*
25	21	17	*Candida albicans*

Table 4 :The inhibition effect of IONPs, blf NPs and blf NP loaded on IONPs in ratio (5%, 10%, 15%) that added to films prepared from (whey protein isolation) in variant type of micro-organism

15%	10%	5%	Micro-Organisms types
16	14	10	*Escherichia coli*
15.5	11	9.5	*Salmonella spp.*
15	12.5	9	*Pseudomonas aeuroginasa*
17	13	11	*Staphylooccus aereus*
14.5	12	10.5	*Bacillus spp*
13.5	10	7	*Candida albicans*

Three forms of prepared nanoparticles have not been properly documented for antimicrobial activity. Together with Gram-positive bacteria, the antibacterial behaviour of iron nanoparticles against Gram-negative bacteria was greater. The disparity in behaviour toward these two kinds of bacteria may be attributed to variations in cell membrane structure and composition [42]. Gram-positive bacteria have thicker membranes of peptidoglycan cells than Gram-negative bacteria [48], rendering penetration of iron nanoparticles more challenging, leading to a low antibacterial answer. The differential susceptibility of bacteria to iron nanoparticles depends on the size of the particles, the composition of the bacterial cell wall,

and the degree of interaction between species and nanoparticles. Lf's antiviral function was also shown in vivo model infections, and proposed for targeted antiviral drug delivery [43]. Research has shown that Lf has multiple functions including iron uptake, anti-bacterial, anti-fungal, anti-viral, cell growth regulation, anti-oxidant, and anti-tumor regulation [45]. Lf has been commonly used in many areas, including food and medicinal applications, inspired by such health-promoting properties [44]. The antioxidant action of phenolic acids is due to their redox characteristics [51]. Free radical scavenging is facilitated by phenols in plant extracts and the presence of certain vitamins, bioactive chemicals, and polyphenols in whey protein. However, the concentration of phenolic compounds in whey has received little attention. The Folin–Ciocalteu reagent was used to determine the phenolic content of the extract and the produced films as a starting point. The results were calculated using a gallic acid (0–1 mg/mL) calibration curve (y=0.07x0.013, R2=0.92) and reported in mg GAE/g of sample (Table 5).

Table 5:Total phenolic contents in the plant extracts and the prepared films expressed in terms of gallic acid equivalent (mg of GAE/ g sample)

Samples	mg of GAE/g sample
Extract	6.6
5% lactoferrin NP loaded IONP film	7.1
10% lactoferrin NP loaded IONP film	7.6
15% lactoferrin NP loaded IONP film	7.9

Table 6 data showed good percentage of antioxidants that the extract and the prepared films contains when compared with vitamin C, which is a strong and effective antioxidant.

Antioxidants are natural ingredients effective for removing the stable purple-colored DPPH radical to the yellow-colored DPPH radical in a visibly detectable manner. The complex's significant DPPH radical scavenging activity was demonstrated in a concentration levels approach in this investigation. The produced films' DPPH radical scavenging activity was greater than those of the extract and lower than that of vit C, the reference antioxidant, at all test concentrations. Bovine WP accounts for 11 to 14.5 percent of powdered whey; the other elements of bovine whey protein are lactose (63–75 percent), fat (1–1.5 percent), minerals (8.2–8.8 percent), and vitamins (A, C, E, and B groups). Whey protein is a comprehensive source of protein that is high in thiol amino acids and branched-chain amino acids (26%). It is composed of β-LG (50–60%), α-LA (15–25%), BSA (6%), lactoferrin (<3%), and immunoglobulins, concluded that the higher reducing power of whey proteins was due to the abundance of lactoferrin and vitamins [52].

Table 6 :DPPH free radical in the plant extracts and the prepared films

Samples	DPPH scavenging effect (%)
Vitamin C	92.99
Extract	70.1
5% lactoferrin NP loaded IONP film	74.59
10% lactoferrin NP loaded IONP film	76.41
15% lactoferrin NP loaded IONP film	79

4. Conclusions

Lactoferrin has traditionally attracted the attentions of scientists as a biological molecule with a broad range of applications. Lactoferrin is an 80-kDa monomeric iron-binding glycoprotein that seems to be the whey subfraction with the most well-documented antiviral, antibacterial, anticancer, and immunological modulating/enhancing properties. Fabrication of lactoferrin packed with IONPS using *CONCARPUS* extraction, including full three-dimensional structural stability, has been accomplished using NPs with whey protein films in this study. The manufactured film did not leach protein after being stored for a long time, demonstrating the efficacy of the nanosized technique. Lactoferrin nanovesicles in whey films made under ideal circumstances were also used effectively in research facility antibacterial and antioxidant studies.

5. Conflicts of interest

There are no conflicts to declare.

6. Acknowledgments

The authors express their gratitude to the Department of Chemistry at Mustansiriyah University for their helpful guiding during the research period.

7. References

[1] Gurdian, C. (2015). "Evaluation of Whey-Protein-Isolate Edible Films Containing Oregano (Origanum vulgare) Essential Oil to Improve Shelf Life of Cheeses During Refrigerated Storage."

[2] Arroyo, B. J., Santos, A. P., de Melo, E. D. A., Campos, A., Lins, L., and BoyanoOrozco, L. C. (2019). “Chapter 8 – Bioactive compounds and their potential use as ingredients for food and its application in food packaging,” in Bioactive Compounds: Health Benefits and Potential Applications, ed. M. R. S. Campos (Sawston:

Woodhead Publishing), 143–156. doi: 10.1016/B978-0-12-814774-0. 00008-6

[3] Bassani, A., Montes, S., Jubete, E., Palenzuela, J., Sanjuan, A. P., and Spigno, G. (2019). Incorporation of waste orange peels extracts into PLA films. Chem. Eng. Trans. 74, 1063–1068. doi: 10.3303/CET1974178

[4] Tong, L. M., et al. (2000). "Mechanisms of the antioxidant activity of a high molecular weight fraction of whey." Journal of Agricultural and Food Chemistry 48(5): 1473-1478.

[5] Chayavanich, K., Thiraphibundet, P., and Imyim, A. (2020). Biocompatible film sensors containing red radish extract for meat spoilage observation. Spectrochim. Acta A. 226, 117601. doi: 10.1016/j.saa.2019.117601

[6] O.U. Igwe, F. Nwamezie (2018) .Green synthesis of iron nanoparticles using flower extract of Piliostigma thonningii and antibacterial activity evaluation .Chem Int, 4, pp. 60-66 .

[7] S. Zinatloo-Ajabshir, M.S. Morassaei, M. Salavati-Niasari (2019) .Facile synthesis of Nd2Sn2O7-SnO2 nanostructures by novel and environment-friendly approach for the photodegradation and removal of organic pollutants in water .J Environ Manage, 233 (2019), pp. 107-119

[8] S. Zinatloo-Ajabshir, M. Salavati-Niasari (2019) .Preparation of magnetically retrievable CoFe2O4@SiO2@ Dy2Ce2O7 nanocomposites as novel photocatalyst for highly efficient degradation of organic contaminants .Compos B Eng (2019), Article 106930

[9] M. Gebrekidan, M. Redi-Abshiro, B.S. Chandravanshi, E. Ele, A.M. Mohammed, H. Mamo (2019) Influence of altitudes of coffee plants on the alkaloids contents of green coffee beans Chem Int, 5 (2019), pp. 247-257 .

[10] Khalil AT, Ovais M, Ullah I, Ali M, Shinwari ZK, Maaza M (2017) Biosynthesis of iron oxide (Fe2O3) nanoparticles via aqueous extracts of Sageretia thea (Osbeck) and their pharmacognostic properties. Green Chem Lett Rev. 10(4):186–201.

[11] Rajiv P, Bavadharani B, Kumar MN, Vanathi P (2017) Synthesis and characterization of biogenic iron oxide nanoparticles using green chemistry approach and evaluating their biological activities. Biocatal Agric Biotechnol 12:45–49.

[12] Kell, D.B.; Heyden, E.L.; Pretorius, E. (2020) .The Biology of Lactoferrin, an Iron-Binding Protein That Can Help Defend Against Viruses and Bacteria. Front. Immunol. 2020, 11, 1221.

[13] Wang, B.; Timilsena, Y.P.; Blanch, E.; Adhikari, B. (2019) .Lactoferrin: Structure, function, denaturation and digestion. Crit. Rev. Food Sci. Nutr. 2019, 59, 580–596.

[14] Wang, B.; Timilsena, Y.P.; Blanch, E.; Adhikari, B. Mild thermal treatment and in-vitro digestion of three forms of bovine lactoferrin: Effects on functional properties. Int. Dairy J. 2017, 64, 22–30.

[15] Chea, C.; Miyauchi, M.; Inubushi, T.; Okamoto, K.; Haing, S.; Thao Nguyen, P.; Imanaka, H.; Takata, T. Bovine lactoferrin reverses programming of epithelial-to-mesenchymal transition to mesenchymal-to-epithelial transition in oral squamous cell carcinoma. Biochem. Biophys. Res. Commun. 2018, 507, 142–147.

[16] Superti, F.; De Seta, F. Warding Off Recurrent Yeast and Bacterial Vaginal Infections: Lactoferrin and Lactobacilli. Microorganisms 2020, 8, 130.

[17] Cutone, A.; Lepanto, M.S.; Rosa, L.; Scotti, M.J.; Rossi, A.; Ranucci, S.; De Fino, I.; Bragonzi, A.; Valenti, P.; Musci, G.; et al. Aerosolized Bovine Lactoferrin Counteracts Infection, Inflammation and Iron Dysbalance in A Cystic Fibrosis Mouse Model of Pseudomonas aeruginosa Chronic Lung Infection. Int. J. Mol. Sci. 2019, 20, 2128.

[18] Drago-Serrano, M.E.; Campos-Rodríguez, R.; Carrero, J.C.; de la Garza, M. Lactoferrin: Balancing Ups and Downs of Inflammation Due to Microbial Infections. Int. J. Mol. Sci. 2017, 18, 501.

[19] Mohammed, M.M.; Ramadan, G.; Zoheiry, M.K.; El-Beih, N.M. Antihepatocarcinogenic activity of whey protein concentrate and lactoferrin in diethylnitrosamine-treated male albino mice. Environ. Toxicol. 2019, 34, 1025–1033.

[20] Ingle KP, Deshmukh AG, Padole DA, Dudhare MS, Moharil MP and Khelurkar V.C. Phytochemicals: Extraction methods, identification and detection of bioactive compounds from plant extracts JPP 2017; 6(1): 32-36.

[21] Saranya, S., et al. (2017). "Green synthesis of iron nanoparticles using aqueous extract of musa ornata flower sheath against pathogenic bacteria." Indian Journal of Pharmaceutical Sciences 79(5): 688-694.

[22] Amutha, S. and S. Sridhar (2018). "Green synthesis of magnetic iron oxide nanoparticle using leaves of Glycosmis mauritiana and their antibacterial activity against human pathogens." Journal of Innovations in Pharmaceutical and Biological Sciences 5: 22-26.

[23] Martins, J. T., et al. (2016). "Lactoferrin-based nanoparticles as a vehicle for iron in food applications–Development and release profile." Food Research International 90: 16-24.

[24] Vandepitte, J., et al. (2003). Basic laboratory procedures in clinical bacteriology, World Health Organization.

[25] Popovi´c, S.Z.; Lazi´c, V.L.; Hromiš, N.M.; Šuput, D.Z.; Bulut, S.N. Chapter 8—Biopolymer Packaging Materials for Food Shelf-Life Prolongation. In Biopolymers for Food Design; Grumezescu, A.M., Holban, A.M., Eds.; AcademicPress: New York, NY, USA, 2018; pp. 223–277

[26] Hassan, B.; Chatha, S.A.S.; Hussain, A.I.; Zia, K.M.; Akhtar, N. Recent advances on polysaccharides, lipids and protein based edible films and coatings: A review. Int. J. Biol. Macromol. 2018, 109, 1095–1107.

[27] Müller, K., et al. (2017). "Modification of functional properties of whey protein isolate nanocomposite films and coatings with nanoclays." Journal of Nanomaterials 2017.

[28] Schmid, M.; Müller, K. Chapter 11—Whey Protein-Based Packaging Films and Coatings. In Whey Proteins; Deeth, H.C., Bansal, N., Eds.; Academic Press: New York, NY, USA, 2019; pp. 407–437.

[29] Maryam Adilah, Z.A.; Jamilah, B.; NurHanani, Z.A. Functional and antioxidant properties of protein-based films incorporated with mango kernel extract for active packaging. Food Hydrocoll. 2018, 74, 207–218.

[30] Mohamed, Y., et al. (2015). "Mycosynthesis of iron nanoparticles by Alternaria alternata and its antibacterial activity." African Journal of Biotechnology 14(14): 1234-1241.

[31] Singleton VL, Orthofer R, Lamuela-Raventos RM: Analysis of total phenols and other oxidation substrates and antioxidants by means of Folin-Ciocalteu reagent. SAN DIEGO, ACADEMIC PRESS INC, 1999.

[32] Devatha, C., et al. (2016). "Green synthesis of iron nanoparticles using different leaf extracts for treatment of domestic waste water." Journal of cleaner production 139: 1425-1435.

[33] Badmapriya, D. and I. Asharani (2016). "Dye degradation studies catalysed by green synthesized Iron oxide nanoparticles." Int. J. ChemTech Res 9: 409-416.

[34] Kanagasubbulakshmi, S. and K. Kadirvelu (2017). "Green synthesis of iron oxide nanoparticles using Lagenaria siceraria and evaluation of its antimicrobial activity." Defence Life Science Journal 2(4): 422-427.

[35] Makarov, V. V., et al. (2014). "Biosynthesis of stable iron oxide nanoparticles in aqueous extracts of Hordeum vulgare and Rumex acetosa plants." Langmuir 30(20): 5982-5988.

[36] Prasad, A.S. 2016 .Iron oxide nanoparticles synthesized by controlled bio-precipitation using leaf extract of garlic vine (Mansoa alliacea). Mater. Sci. Semicond. Process., 53, 79–83.

[37] Lim, L. Y., et al. (2015). "Tumor regression following intravenous administration of lactoferrin-and lactoferricin-bearing dendriplexes." Nanomedicine: Nanotechnology, Biology and Medicine 11(6): 1445-1454.

[38] ATHMAKUR, H. and A. K. KONDAPI (2018). "CARMUSTINE LOADED LACTOFERRIN NANOPARTICLES DEMONSTRATES AN ENHANCED ANTIPROLIFERATIVE ACTIVITY AGAINST GLIOBLASTOMA IN VITRO." Int J App Pharm 10(6): 234-241.

[39] Kadam, D. M., et al. (2013). "Preparation and characterization of whey protein isolate films reinforced with porous silica coated titania nanoparticles." Journal of food engineering 117(1): 133-140.

[40] Kavoosi, G., et al. (2013). "Mechanical, physical, antioxidant, and antimicrobial properties of gelatin films incorporated with thymol for potential use as nano wound dressing." Journal of food science 78(2): E244-E250.

[41] Murrieta-Martínez, C.L.; Soto-Valdez, H.; Pacheco-Aguilar, R.; Torres-Arreola, W.; Rodríguez-Felix, F.; MárquezRíos, E. Edible protein films: Sources and behavior. Packag. Technol. Sci. 2018, 31, 113–122.

[42] Ananey-Obiri, D.; Matthews, L.; Azahrani, M.H.; Ibrahim, S.A.; Galanakis, C.M.; Tahergorabi, R. Application of protein-based edible coatings for fat uptake reduction in deep-fatfried foods with an emphasis on muscle food proteins. Trends Food Sci. Technol. 2018, 80, 167–174. [

[43] Farhan, A.; Hani, N.M. Characterization of edible packaging films based on semi-refined kappa-carrageenan plasticized with glycerol and sorbitol. Food Hydrocoll. 2017, 64, 48–58

[44] Nicolai, T. and D. Durand (2013). "Controlled food protein aggregation for new functionality." Current Opinion in Colloid & Interface Science 18(4): 249-256.

[45] Adlerova, L., et al. (2008). "Lactoferrin: a review." Veterinarni Medicina 53(9): 457-468.

[46] Bourbon, A. I., et al. (2015). "Development and characterization of lactoferrin-GMP nanohydrogels: Evaluation of pH, ionic strength and temperature effect." Food Hydrocolloids 48: 292-300.

[47] Padil, V. V. T. and M. Černík (2013). "Green synthesis of copper oxide nanoparticles using gum karaya as a biotemplate and their antibacterial application." International journal of nanomedicine 8: 889.

[48] Liu, J., et al. (2011). "Magnetic nanocomposites with mesoporous structures: synthesis and applications." Small 7(4): 425-443.

[49] Yang, Z., et al. (2018 " (Concentration of lactoferrin in human milk and its variation during lactation in different Chinese populations." Nutrients 10(9): 1235.

[50] González-Chávez, S. A., et al. (2009). "Lactoferrin: structure, function and applications." International journal of antimicrobial agents 33(4): 301. e301-301. e308.

[51] F. Shahidi and M. Naczk, “Antioxidant Properties of Food Phenolics,” In: F. Shahidi and M. Naczk, Eds., Phenolics in Food and Nutraceuticals, CRC Press, Boca Raton, 2003, pp. 1-403.

[52] W. Brand-Williams, M. E. Cuvelier and C. Berset, “Use of a Free Radical Method to Evaluate Antioxidant Activ- ity,” LWT—Food Science and Technology, Vol. 28, No. 1, 1995, pp. 25-30.